Electric-Potential Reconstructions of Single Particles Using L^2-Gradient Flows

Ming Li*, Guoliang Xu*§, Carlos O. S. Sorzano†, Roberto Melero† and Chandrajit Bajaj‡
*State Key Laboratory of Scientific and Engineering Computing
Institute of Computational Mathematics, Academy of Mathematics and
System Sciences, Chinese Academy of Sciences, Beijing 100190, China
†Biocomputing Unit, Centro Nacional de Biotecnologia (CSIC)
Campus Univ. Autonoma 28049, Cantoblanco - Madrid
‡Department of Computer Sciences and Institute of Computational
Engineering & Sciences, University of Texas at Austin, Austin TX 78712

***Abstract*—In this paper, we present a stable, reliable and robust method for reconstructing a three dimensional density function from a set of two dimensional electron microscopy images. By minimizing an energy functional consisting of a fidelity term and a regularization term, a L^2-gradient flow is derived. The flow is integrated by a finite element method in the spatial direction and an explicit Euler scheme in temporal direction. The experimental results show that the proposed method is efficient and effective.**

I. Introduction

In the past few years, cryo-electron microscope imaging techniques have established themselves as indispensable tools for determining the three dimensional(3D) structures of large macromolecules and biological machineries. The pipeline of single-particle techniques includes particle picking, classification and alignment, orientation and reconstruction [3], [8], [10]–[12].

The usually used reconstruction algorithms are filtered back projection(FBP) [7], direct fourier reconstruction [7], and iterative methods including algebraic reconstruction technique(ART) [5], simultaneous iterative reconstructive technique(SIRT) [4], and simultaneous algebraic reconstruction technique(SART) [2]. In order to accelerate convergence of these algorithms block iterative techniques have been proposed [5], [6].

In this paper, we propose a volume constraint algorithm which assumes the volume of the object would be a prior knowledge and keep unchanged during the imaging process. Besides, we propose a new variational reconstruction method which employs the level set and L^2 gradient flow technique [13] with volume-preserving regularization. Our method is a series expansion method. Assume the object f has a mathematical expression. Instead of using pixel basis functions, we use tri-cubic B spline basis functions. f can be expressed as a linear combination of these B spline basis functions. One of the advantages of using B spline basis functions is that we can obtain a C^2 smooth object. And the local support property of B splines can be used to accelerate the reconstruction process. We use a finite element method (FEM) to solve the variational problem. To avoid solving large linear equations, orthogonalization of B spline basis functions will be employed.

The rest of these paper is organized as follows. In Section 2 some basic setting is defined including image size, B spline basis function grid and volume grid. Section 3 explains our algorithms in details. Section 4 gives some illustrative examples. Finally, we conclude this paper in Section 5.

§Corresponding author email: xuguo@lsec.cc.ac.cn.

II. Problem Setting

Let $\{g_{\mathbf{d}}\}$ be a set of the two-dimensional images measured from an unknown three-dimensional function (electric-potential) f by X-ray projection $X_{\mathbf{d}}$ in the direction $\mathbf{d} \in S^2$. Our problem is to construct $f(x,y,z)$, $(x,y,z)^T \in \Omega \subset \mathbf{R}^3$, such that $X_{\mathbf{d}} f$ is as close to $g_{\mathbf{d}}$ as possible.

We assume all the measured images have the same size $(n+1)\times(n+1)$, the pixel values $g_{\mathbf{d}}$ of each image are defined on the integer grid points $(i,j)^T \in \left[-\frac{n}{2},\frac{n}{2}\right]^2$ (we assume n is an even number). Since $g_{\mathbf{d}}$ is the projection of f, we therefore define Ω as

$$\Omega = \left\{(x,y,z)^T : \sqrt{x^2+y^2+z^2} \le \frac{n}{2}+1\right\}.$$

For simplicity, we put this sphere within a cube defined as $\Omega_c = \left[-\frac{n}{2}-1,\frac{n}{2}+1\right]^3$, with the assumption that

$$\begin{aligned} f(x,y,z) &= 0 \quad \text{if} \quad (x,y,z)^T \in \Omega_c \setminus \Omega, \\ g_{\mathbf{d}}(i,j) &= 0 \quad \text{if} \quad \sqrt{i^2+j^2} > \frac{n}{2}. \end{aligned}$$

Let $\mathbf{d} \in S^2$. The image values $g_{\mathbf{d}}$ at the grid points are defined as

$$g_{\mathbf{d}}(i,j) = \int_{-\infty}^{\infty} f(i\mathbf{e}_{\mathbf{d}}^{(1)} + j\mathbf{e}_{\mathbf{d}}^{(2)} + t\mathbf{d})\,\mathrm{d}t, \quad (i,j)^T \in \left[-\frac{n}{2},\frac{n}{2}\right]^2$$

for the unknown function f, where $\mathbf{e}_{\mathbf{d}}^{(1)}$ and $\mathbf{e}_{\mathbf{d}}^{(2)}$ are two directions satisfying

$$\|\mathbf{e}_{\mathbf{d}}^{(1)}\| = \|\mathbf{e}_{\mathbf{d}}^{(2)}\| = 1, \quad \langle \mathbf{e}_{\mathbf{d}}^{(1)}, \mathbf{e}_{\mathbf{d}}^{(2)} \rangle = 0, \tag{1}$$

$$\langle \mathbf{e}_{\mathbf{d}}^{(1)}, \mathbf{d} \rangle = 0, \quad \langle \mathbf{e}_{\mathbf{d}}^{(2)}, \mathbf{d} \rangle = 0. \tag{2}$$

$\mathbf{e}_{\mathbf{d}}^{(1)}$ and $\mathbf{e}_{\mathbf{d}}^{(2)}$ also determine the in-plane rotation.

Given an even and positive integer $m = 2l$, let $h = \frac{n+2}{m}$, and the domain Ω_c is uniformly partitioned with grid point $(i, j, k)h$ for $(i, j, k) \in [-l, l]^3$. The function f is represented as

$$f(x, y, z) = \sum_{i=-l+2}^{l-2} \sum_{j=-l+2}^{l-2} \sum_{k=-l+2}^{l-2} f_{ijk} N_i^3(x) N_j^3(y) N_k^3(z), \tag{3}$$

where $(x, y, z)^T \in \Omega_c$, N_α^3 are cubic B-spline basis functions defined on the interval $[-2h + \alpha h, 2h + \alpha h]$.

To reconstruct the electric-potential in the spatial domain, we minimize the following energy functional.

$$J(f) = J_1(f) + \alpha J_2(f) + \beta J_3(f), \tag{4}$$

where

$$\begin{aligned} J_1(f) &= \int_{S^2} \int_{\mathbf{R}^2} \left(X_{\mathbf{d}} f - g_{\mathbf{d}}\right)^2 \mathrm{d}u\mathrm{d}v\mathrm{d}A, \\ J_2(f) &= \int_{\Gamma_c} g(H, K)\mathrm{d}A, \\ J_3(f) &= \int_{\mathbf{R}^3 \setminus \Omega_{\Gamma_c}} f(\mathbf{x})^2 \mathrm{d}\mathbf{x}, . \end{aligned}$$

In J_1, $X_{\mathbf{d}}$ stands for a projection of a 3D function in the direction $\mathbf{d} \in S^2$. $\Gamma_c = \{\mathbf{x} \in \mathbf{R}^3 : f(\mathbf{x}) = c\}$ in J_2, J_3 is an iso-surface of f, c is a given constant and Ω_{Γ_c} is the region enclosed by Γ_c. Here $\mathcal{H}(f)$ denotes the Hessian matrix of f. H and K stand for the mean and Gaussian curvatures of surface Γ_c.

1) Obviously, J_1 is used to minimize the error of the measured images and the reconstructed images.
2) J_2 is a regularization term that makes the iso-surface Γ_c smooth in certain sense, depending on the type of function g that is used. We usually take $g(H, K) = 1$ or $g(H, K) = \|\nabla f\|$.
3) J_3 is used to make the reconstructed function as close to zero (background density) as possible outside the volume Ω_{Γ_c}, so that there are no outliers.

Algorithm Steps. Since Γ_c depends on f, the energy functional $J(f)$ is nonlinear with respect to f. To minimize $J(f)$, we use the following iterative algorithm:

1) Given an initial f.
2) Determine the constant c.
3) Minimize $J(f)$ by changing f.
4) Checking the termination conditions $|J(f^{(k+1)}) - J(f^{(k)})| < \epsilon$. If they are satisfied, stop the iteration, otherwise repeat from step 2.

In the next section, we explain each of the steps in some details.

III. Implementation Details

A. Estimate Iso-value c

For an electric-potential density function $f \in \mathbf{R}^3$ for a protein, we need to select an iso-value c, so that the iso-surface Γ_c is the boundary (molecular surface) of the protein. We determine c such that

$$\mathrm{card}\{\mathbf{x}_{ijk} : f(\mathbf{x}_{ijk}) > c\} = V_0/V_{cube},$$

where card stands for the cardinality of a finite set, V_{cube} is the volume of the voxel. Hence, we first sort $f(\mathbf{x}_{ijk})$ in decreasing order:

$$g_1 \geq g_2 \geq \cdots,$$

and select g_n as the isovalue c, where n is the integer part of V_0/V_{cube}.

B. Updating f

We wish to minimize $J(f)$ by adjusting f. This goal is achieved by solving a L^2-gradient flow of $J(f)$ in the B-spline space. Let us first construct the flow. Based on Variational methods and Green formula, it is easy to derive the following first order variational form.

$$\delta(J_1(f), \psi) = 2 \int_{S^2} \int_{\mathbf{R}^2} (X_{\mathbf{d}} f - g_{\mathbf{d}}) X_{\mathbf{d}} \psi \mathrm{d}u\mathrm{d}v\mathrm{d}A.$$

If $g(H, K) = 1$, $\delta(J_2(f), \psi)$ is computed by

$$\delta(J_2(f), \psi) = -\int_{\mathbf{R}^3} \mathfrak{6}(f - c)\mathrm{div}\left(\frac{\nabla f}{\|\nabla f\|}\right)\psi \mathrm{d}\mathbf{x}.$$

If $g(H, K) = \|\nabla f\|$, then we have

$$\delta(J_2(f), \psi) = 2 \int_{\mathbf{R}^3} \mathfrak{6}(f - c)\nabla f \nabla \psi \mathrm{d}\mathbf{x},$$

Where $\mathfrak{6}$ denotes delta function. In this paper, we use the following approximation.

$$\mathfrak{6}_\alpha(x) = \begin{cases} 0, & |x| > \alpha, \\ \frac{1}{2\alpha}\left[1 + \cos\left(\frac{\pi x}{\alpha}\right)\right], & |x| \leq \alpha, \end{cases} \tag{5}$$

where $\alpha > 0$ is a given parameter, which control the support $[-\alpha, \alpha]$ of $\mathfrak{6}_\alpha(x)$. Note that $\mathfrak{6}_\alpha(x)$ is a C^1 smooth function.

$$\delta(J_3(f), \psi) = \int_{\mathbf{R}^3} [\mathfrak{6}(c - f) f^2 \psi + 2\mathrm{H}(c - f) f \psi] \mathrm{d}\mathbf{x},$$

Using these first order variations, we construct the following weak form L^2-gradient flow.

$$\int_{\mathbf{R}^3} \frac{\partial f}{\partial t} \psi \mathrm{d}\mathbf{x} + \delta(J_1(f), \psi) + \alpha\delta(J_2(f), \psi) + \beta\delta(J_3(f), \psi) = 0, \tag{6}$$

for all ψ in the B-spline function space. We solve (6) using a numerical method. In the temporal discretization, we use an explicit forward Euler scheme. For the spatial direction discretization we use finite element method. These discretization lead to a linear system, which are solved using direct method.

C. Finite Element Discretization

Denote $\mathbf{x} = [x, y, z]^T$, suppose

$$f(\mathbf{x}) = \sum_i \sum_j \sum_k f_{ijk} N_i^{(1)}(x) N_j^{(2)}(y) N_k^{(3)}(z), \quad (7)$$

with f_{ijk} as unknowns, and $N_\alpha^{(p)} = N_\alpha^3, p = 1, 2, 3$. Taking the test function ψ as $\phi_{i'j'k'}(\mathbf{x}) = N_{i'}^{(1)}(x) N_{j'}^{(2)}(y) N_{k'}^{(3)}(z)$, we then obtain a matrix form

$$MX = B$$

for (6). The elements of matrix M are in the form

$$\int_{\mathbf{R}} N_i^{(1)} N_{i'}^{(1)} \mathrm{d}x \int_{\mathbf{R}} N_j^{(2)} N_{j'}^{(2)} \mathrm{d}y \int_{\mathbf{R}} N_k^{(3)} N_{k'}^{(3)} \mathrm{d}z.$$

The one-dimensional integrals above can be computed by a Gauss quadrature formula (see [1], [14]). The elements of the vector B are

$$-[\delta(J_1(f), \phi_{i'j'k'}) + \delta(J_2(f), \phi_{i'j'k'}) + \delta(J_3(f), \phi_{i'j'k'})].$$

The computations involving delta function are computed in the neighborhood of surface Γ_c. This does not mean we need to have an explicit representation for Γ_c. What we need is the $\mathfrak{d}(f - c)$, which is approximated by $\mathfrak{d}_\alpha(f - c)$ (see (5)).

1) Fast Computation of Stiff Matrix M: We orthogonalize the basis functions $N_i^{(l)}(x)$ using the Schimidt orthogonalization process, to obtain new basis functions $\tilde{N}_i^{(l)}(x)$, such that

$$\int_{\mathbf{R}} \tilde{N}_i^{(l)}(x) \tilde{N}_j^{(l)}(x) \mathrm{d}x = \delta_{ij}, \quad i, j = 1, \cdots, n, \quad l = 1, 2, 3.$$

Let

$$\tilde{\phi}_{ijk} = \tilde{N}_i^{(1)} \tilde{N}_j^{(2)} \tilde{N}_k^{(3)}.$$

Then by representing the function f using the new basis $\tilde{\phi}_{ijk}$, we obtain a unit matrix M. Hence there is no need to store and inverse the matrix.

Now we have representation (7) of f and the representation

$$f(\mathbf{x}) = \sum_i \sum_j \sum_k \tilde{f}_{ijk} \tilde{N}_i^{(1)}(x) \tilde{N}_j^{(2)}(y) \tilde{N}_k^{(3)}(z). \quad (8)$$

2) Fast Computation of $\delta(J_1, \psi)$: Consider the computation of the term $\delta(J_1(f), \psi)$ in (6). Using (7) and taking $\psi = \tilde{\phi}_{i'j'k'}$, we have

$$\begin{aligned} &\delta(J_1(f), \tilde{\phi}_{i'j'k'}) \\ &= 2 \int_{S^2} \int_{\mathbf{R}^2} (X_{\mathbf{d}} f - g_{\mathbf{d}}) X_{\mathbf{d}} \tilde{\phi}_{i'j'k'} \mathrm{d}u\mathrm{d}v\mathrm{d}A \quad (9) \\ &\approx 2 \int_{S^2} \int_{-\frac{n}{2}}^{\frac{n}{2}} \int_{-\frac{n}{2}}^{\frac{n}{2}} (X_{\mathbf{d}} f - g_{\mathbf{d}}) X_{\mathbf{d}} \tilde{\phi}_{i'j'k'} \mathrm{d}u\mathrm{d}v\mathrm{d}A. \quad (10) \end{aligned}$$

Now let us explain how each of the terms in (10) is efficiently computed.

Computing $X_{\mathbf{d}} \tilde{\phi}_{i'j'k'}$.

First consider the computation of $X_{\mathbf{d}} \tilde{\phi}_{i'j'k'}$. The computation mainly includes two steps:

1) Compute $X_{\mathbf{d}} \phi_{ijk}$ for all i, j, k.

2) Convert $X_{\mathbf{d}} \phi_{ijk}$ to $X_{\mathbf{d}} \tilde{\phi}_{i'j'k'}$.

Since the second step is straightforward, we describe only the first one in detail. Let $\mathbf{d} \in S^2$ be a given direction. Then the projection of ϕ_{ijk} in the direction $\mathbf{d}$ is a two-dimensional function, defined as

$$\begin{aligned} &(X_{\mathbf{d}} \phi_{ijk})(u, v) \\ &= \int_{-\infty}^{\infty} \phi_{ijk}(u\mathbf{e}_{\mathbf{d}}^{(1)} + v\mathbf{e}_{\mathbf{d}}^{(2)} + t\mathbf{d}) \, \mathrm{d}t, \\ &= \int_{-\infty}^{\infty} N_i^3([u, v, t]\mathbf{a}_1) \, N_j^3([u, v, t]\mathbf{a}_2) N_k^3([u, v, t]\mathbf{a}_3) \, \mathrm{d}t, \end{aligned}$$

where $\mathbf{e}_{\mathbf{d}}^{(1)}$ and $\mathbf{e}_{\mathbf{d}}^{(2)}$ are two directions defined by (1), which spans the (u, v)-plane in space $\mathbf{R}^3$, $[\mathbf{a}_1, \mathbf{a}_2, \mathbf{a}_3] = [\mathbf{e}_{\mathbf{d}}^{(1)}, \mathbf{e}_{\mathbf{d}}^{(2)}, \mathbf{d}]^T$.

Computing $X_{\mathbf{d}} f$.

Here we propose an efficient approach for computing $X_{\mathbf{d}} f$. Since

$$X_{\mathbf{d}} f = X_{\mathbf{d}} \sum_{ijk} f_{ijk} \phi_{ijk} = \sum_{ijk} f_{ijk} X_{\mathbf{d}} \phi_{ijk},$$

and since $X_{\mathbf{d}} \phi_{ijk}$ have been computed previously, $X_{\mathbf{d}} f$ is easily computed from $X_{\mathbf{d}} \phi_{ijk}$. Notice that $X_{\mathbf{d}} \phi_{ijk}$ is locally supported. The cost for computing $X_{\mathbf{d}} f$ is $O(n^3)$. The total cost for the projection is $O(pn^3)$,where p denotes the total number of projections.

D. Temporal Step-size

It is obvious that using a too small time step-length will slow down the evolution process, while on the contrary using a too large time step-length has the danger of causing the evolution blow up. Hence, choosing a suitable time step-length is crucial to efficiently reconstruct the function. From the L^2 gradient flow (6), we can see that after one step iteration, the function f is updated as

$$f = f^{(p)} + \tau \Delta f,$$

where $f^{(p)}$ is the function at previous step, Δf is the increment of $f^{(p)}$ computed using the L^2 gradient flow. The problem here is how large the temporal size τ should be used. We determine τ such that

$$\int_{S^2} \int_{\mathbf{R}^2} \left[X_{\mathbf{d}}(f^{(p)} + \tau \Delta f) - g_{\mathbf{d}} \right]^2 \mathrm{d}u\mathrm{d}v\mathrm{d}A = min.$$

From this we can easily derive that the best τ we should choose is

$$\tau = - \frac{\int_{S^2} \int_{\mathbf{R}^2} \left[X_{\mathbf{d}}(f^{(p)}) - g_{\mathbf{d}} \right] X_{\mathbf{d}}(\Delta f) \mathrm{d}u\mathrm{d}v\mathrm{d}A}{\int_{S^2} \int_{\mathbf{R}^2} [X_{\mathbf{d}}(\Delta f)]^2 \, \mathrm{d}u\mathrm{d}v\mathrm{d}A}.$$

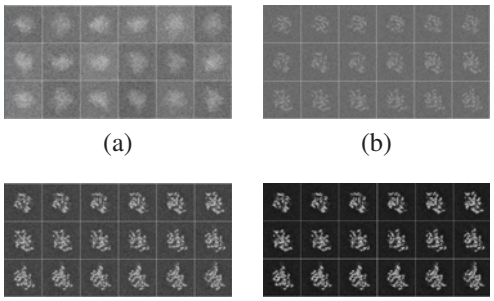

Fig. 1. (a) 2D noisy projections of 1FFK. (b) reconstructed result using J_1. (c) reconstructed result using $J_1 + J_2$. (d) reconstructed result using $J_1 + J_2 + J_3$.

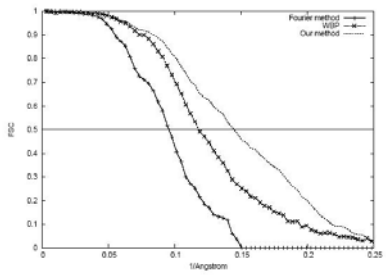

Fig. 2. Fourier shell correlation curves of 1FFK.

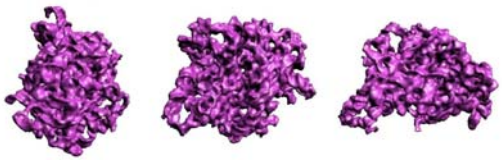

Fig. 3. Reconstructed 1FFK Volume. From left to right: Side view; Side view; Top view;

IV. Illustrative Examples

A. Simulated Data

We first applied our algorithm to a large ribosomal subunit(PDB-ID=1FFK). This data contained 5000 projections with random projection directions. The image size was 143×143 with $2.8\mathring{A}$ pixel size. Part of the projections were shown in Fig. 1(a).

We use the algorithm with J_1 term, J_1+J_2 and $J_1+J_2+J_3$ respectively. Fig. 1(b), (c) and (d) show part of the slices along the $z-$ axis of the reconstructed functions. From these pictures we can easily see that the result using $J_1+J_2+J_3$ have higher contrast and lower noise.

Furthermore, we randomly split the data set in two equal parts, reconstructed two volumes using the two subsets respectively and computed the resolution using Fourier shell correlation(FSC) function with 0.5 cutoff. We compared our result using $J_1 + J_2 + J_3$ with WBP and Fourier methods. It is easily seen from Fig. 2 that our method can achieve better resolution than WBP and Fourier's. A 3D volume iso-value surface was shown in Fig. 3.

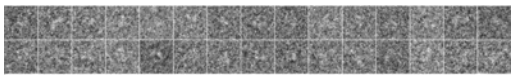

Fig. 4. Noisy projections of p53.

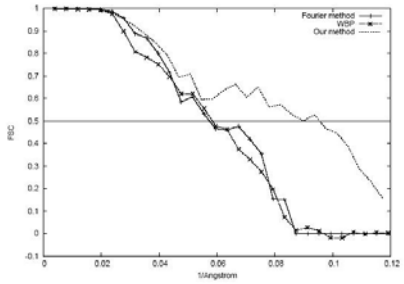

Fig. 5. FSC curves of p53.

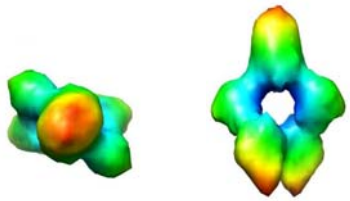

(a) (b)

Fig. 6. Reconstructed p53 volume.(a) (b): Views from different side.

3800 independent projections that thanks to the C2 symmetry yield 7600 projections

B. Experimental Data

Our second experiment use a data set contained 3800 independent projections of a mutant of p53 that thanks to the C2 symmetry yield 7600 projections. This molecule has a C2 symmetry along the principle axis($z-$axis). Fig. 4 shows part of the 2D noisy projections.

In this experiment, we first computed three functions using $J_1+J_2+J_3$ with three different regularization terms $g(\mathbf{x}) = 0$ (means no regularizer), $g(\mathbf{x}) = \|\nabla f(\mathbf{x})\|$ and $g(\mathbf{x}) = 1$ respectively. For each case, we calculated its FSC and resolution. These results were put into table I.

TABLE I
Resolution compare with different regularization terms.

	$g = 0$	$g = \|\nabla f\|$	$g = 1$
FSC	0.052	0.085	0.068
Resolution	19.23Å	11.76Å	14.71Å

In this table, the best resolution was obtained by using regularization term $g = \|\nabla f\|$.

Next, we reconstructed the p53 3D volume using $J_1 + J_2 + J_3$ with regularization term $g = \|\nabla f\|$, WBP and Fourier method respectively. From Fig. 5, we can see that our method using $J_1 + J_2 + J_3$ obtained the best resolution(10.48Å). This reconstructed volume was shown in Fig. 6.

Finally, we applied our algorithm to a virus named as Adenovirus (see [9] for the data) with icosahedral symmetry.

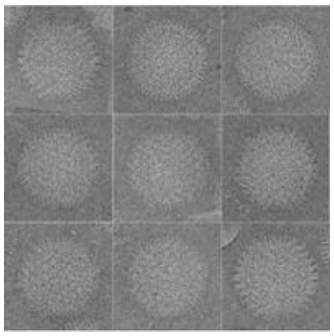

Fig. 7. Part of the noisy projections of Adenovirus.

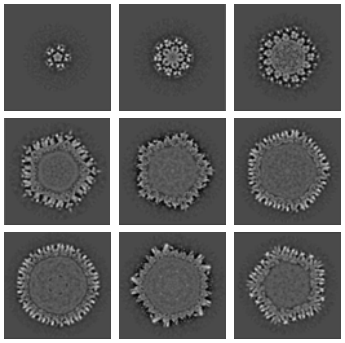

Fig. 8. Part of the slices along the $z-$axis of reconstructed Adenovirus.

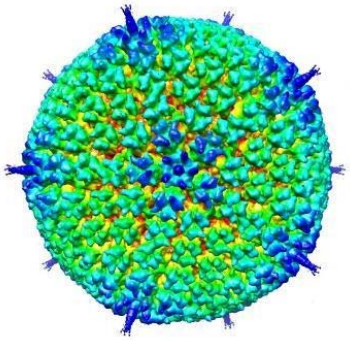

Fig. 9. Reconstructed volume of Adenovirus.

This data set contained 9621 noisy projections(See Fig. 7) with image size 408×408. J_1, J_2 and J_3 were used to reconstruct the three dimensional volume function. Part of the slices along the $z-$axis of the reconstructed volume and iso-surface rendering were shown in Fig. 8 and 9 respectively. These resolutions are 8.73Å for our method, 10.24Å for Fourier method and 10.48 Å for WBP.

V. Conclusions

In this paper, we proposed a new 3D single particle reconstruction algorithm using L^2 gradient flow. We employed the minimal support property of B-spline and Schmidt orthogonalization process to accelerate the algorithm. In the end, simulated and experimental experiments show our algorithm using regulation term $g = \|\nabla f\|$ could achieve the best resolution compared with WBP and Fourier method.

Acknowledgment

We hereby thank Carmen San Martin of Biocomputing Unit, Centro Nacional de Biotecnologia (CSIC), Madrid for his courtesy of affording Adenovirus data. Guoliang Xu was supported in part by NSFC under the grant 60773165, NSFC key project under the grant 10990013. Chandrajit Bajaj was supported by NIH contracts R01-EB004873, R01-GM074258.

References

[1] M. Abramowitz and I. A. Stegun. *Handbook of Mathematical Functions with Formulas, Graphics, and Mathematical Tables*. America Dover Publications, Inc., 1972.

[2] A. H. Andersen and A. C. Kak. Simultaneous algebraic reconstruction technique (sart): A superior implementation of the art algorithm. *Ultrason Imaging.*, 6(1):81–94, 1984.

[3] R. A. Crowther. Procedures for three-dimensional recnostruction of spherical viruses by fourier sythesis from electron micrographs. *Phil. Trans. R. Soc. Lond.*, B(261):221–230, 1971.

[4] P. Gilbert. Iterative methods for the three-dimensional reconstruction of an object from projections. *Journal of Theoretical Biology*, 36(1):105–117, 1972.

[5] R. Gordon, R. Bender, and G. T. Herman. Algebraic reconstruction techniques (art) for three-dimensional electron microscopy and x-ray photography. *J. Theoretical Biology*, 29:471–481, 1970.

[6] R. Marabini, G. T. Herman, and J. M. Carazo. 3d reconstruction in electron microscopy using art with smooth spherically symmetric volume elements (blobs). *Ultramicroscopy*, 72:53–65, 1998.

[7] F. Natterer and Frank Wübbeling. *Mathematical Methods in Image Reconstruction*. SIAM, Philadelphia, 2001.

[8] P. A. Penczek, R. A. Grasucci, and J. Frank. The ribosome at improved resolution: New techniques for merging and orientation refinement in 3d cryo-electron microscopy of biological particles. *Ultramicroscopy*, 53:251–270, 1994.

[9] A. J. Pérez-Berná, R. Marabini, S. H. W. Scheres, R. Menéndez-Conejero, I. P. Dmitriev, D. T. Curiel, W. F. Mangel, S. J. Flint, and C. San Martìn. Structure and uncoating of immature adenovirus. *Journal of Molecular Biology*, 392(2):547–557, 2009.

[10] M. Radermacher. Three-dimensional reconstruction from random projections–orientational alignment via radon transforms. *Ultramicroscopy*, 53:121–136, 1994.

[11] C. O. S. Sorzano, S. Jonic, C. El-Bez, J. M. Carazo, S. De Carlo, P. Thévennaz, and M. Unser. A multiresolution approach to pose assignment in 3-d electron microscopy of single particles. *J. Structural Biology*, 146:381–392, 2004.

[12] M. van Heel. Angular reconstruction: a posteriori assignment of projection directions for 3d reconstruction. *Ultramicroscopy*, 21:111–124, 1987.

[13] G. Xu. *Geometric partial differential equation methods in computational geometry*. Science Press, Beijing, 2008.

[14] G. Xu and Y. Shi. Progressive computation and numerical tables of generalized Gaussian quadrature formulas. *Journal on Numerical Methods and the Computer Application*, 27(1):9–23, 2006.